

Experiment analysis of non-uniformity measurement by array detector scanning system

Napat Watjanatepin¹, Patcharanan Sritanauthaikorn², Chaiyant Boonmee²,
Paiboon Kiatsookkanatorn³, Sarayoot Thongkullaphat², Suvina Sodajaroen⁴

¹Research Section, Research and Development Institute, Rajamangala University of Technology Suvarnabhumi,
Phranakhon Si-Ayutthaya, Thailand

²Department of Electrical Engineering, Rajamangala University of Technology Suvarnabhumi, Nonthaburi, Thailand

³Department of Electrical Engineering, Rajamangala University of Technology Suvarnabhumi, Samchuk, Suphanburi, Thailand

⁴Department of Industrial Engineering, Rajamangala University of Technology Suvarnabhumi, Samchuk, Suphanburi, Thailand

Article Info

Article history:

Received Jun 17, 2022

Revised Aug 30, 2022

Accepted Sep 13, 2022

Keywords:

Array scanning device

Non-uniformity

Photodiode

Solar simulator

Uncertainty

ABSTRACT

Solar simulator is used to analysis characteristic of the solar cells. The non-uniformity is its major performance. The traditional non-uniformity measurement calls single detector method. The paper's objective is to design and construct an array detector scanning system and to determine the optimal scanning time to achieve the lowest uncertainty. To investigate the non-uniformity by our proposed method and the traditional method, our detector consisted of eight photodiodes mounted on an arm of a linear motion lead screw to guide the detector scanning onto the lighting area. A microcontroller applied for controlling and measuring light irradiance in 64 points corresponding to IEC 60904-9 standard. The results showed that the array detector scanned at a speed of 33.33 mm/s to obtain the non-uniformity with the lowest uncertainty, less than 0.6%. Analysis results of the non-uniformity obtained from our system on the test areas of (mm×mm) 156×156, 166×166 and 200×200 compared with the single detector. It showed that the mean absolute error was 1.27. Our system provided a lower uncertainty than the traditional method. The measurement accuracy was acceptable. The advantage is for testing on different test areas within a single device. The measurement time is around 1/32 of the traditional method.

This is an open access article under the [CC BY-SA](https://creativecommons.org/licenses/by-sa/4.0/) license.



Corresponding Author:

Patcharanan Sritanauthaikorn

Department of Electrical Engineering, Rajamangala University of Technology Suvarnabhumi

217 Suanyai, Muang, Nonthaburi, 11000, Thailand

Email: patcharanan.s@rmutsb.ac.th

1. INTRODUCTION

The solar simulator used to test the photovoltaic module is divided into two types: steady state solar simulator and flash solar simulator. Each type is applied and different structures such as the flash type is suitable for testing equipment with time invarian, for instant, the testing of I-V characterisation of photovoltaic module [1]. The steady state solar simulator is suitable for testing materials used in the production of solar cells made of semiconductor materials that have a longer response time than silicon crystals. It is suitable for indoor solar collector testing and other material testing and so on [2].

Performance of the solar simulator is guided by the standard of IEC 60904-9, ASTM E927 and JIS C8912. This includes spectral mismatch, spatial non-uniformity, and temporal instability [3]. Spectral mismatch means that how much the spectrum of artificial light is consistent with the solar spectrum. This is calculated from the percentage of the spectrum divided into each wavelength range versus the reference value. Temporal instability is the irradiance amplitude of artificial lights that variations over time [2].

Spatial non-uniformity is an index that shows the homogeneity of the light source. Non-uniformity is one of the most difficult parameters to design of a solar simulator to provide good non-uniformity value. This value is very important because it affects the efficiency of the photovoltaic module. When the irradiance over the photovoltaic module is uneven, the efficiency of converting light energy to electricity is decreased [4]–[6]. The uniformity of the light source of the beam avoids the effect of shadows on the solar panels, causing some cells to act as resistors rather than power generators [7].

The measurement of the non-uniformity by using light detector is divided into 2 methods: i) Using a single detector; this is a traditional method may use single photo detector devices such as solar cells/photodiodes or pyranometer [1], [8]. Single detector captures and scans light intensity at various locations on the test area [9]. It is appropriate for steady state non-uniformity [1], [2], [10], [11]. The advantages of this method are easy to measure and not complicated because it uses only one photo detector. It can also be easily measured on different areas by only changing the position of the photo detector. The disadvantage is given more uncertainty of the measurement. The temperature may affect to measure inaccurately. Lastly, it takes a long time to keep a measured data [12]; ii) Using an array detector; it uses multiple photodetectors. In general, the number of photo detectors is equal to the number of measured points. This method measures light on a single test plane, so it is suitable for uniformity of the flash solar simulator. Measurement with an array detector has more advantage in measuring time, high speed [13]–[17]. The uncertainty of measurement is the lowest, compared to the single detector [12]. However, there is also a disadvantage. It is a complex measurement system, since measuring with multiple photo detectors. All photo detectors must be calibrated to no different light response. The dimension of the array detector is fixed, so it cannot be applied to measured on various test plane dimension.

From the above mentioned reasons, the research questions, therefore, arises as following. Is there any uniformity measuring system that can measure faster and give better uncertainty of measurement than using a single detector? Can it also measure on different size of exposure areas? Of course, the automated moving system will solve the problems of the research presented here.

Here, the authors will investigate the non-uniformity measurement by scanning of a photo detector's array. The scanning-array measurement method is appropriate for the steady state solar simulator by using the array detector moving with robotic technology. The objective of this research was to design and construct an array detector scanning system and find out the optimal scanning time to achieve the lowest uncertainty of the measurement. Also, Comparating the non-uniformity of irradiance between the proposed method and a single detector method was presented. The novelty of this system is that it can measure non-uniformity on the various sizes of test plane without changing the photo detectors.

2. METHOD

2.1. Design goal

This device was consisted of one set of array detector which included eight photo sensors installed in a longitudinal line. The motion of the array detector was on a linear slide based. The movement of device was controlled by a microcontroller. It covered a test area according as dimensions of mono-crystalline solar cell (wafer size; M0 to M10 of 156×156 mm to 200×200 mm), which corresponds to the currently widely used for the standard solar cell [13]. When an array detector scanning system was applied, the light measurement on the exposure area to obtain 64 irradiance data following to the non-uniformity measurement method of IEC 60904-9 [2], [3], [15]. Measured data was transmitted to a digital file in memory card and subsequently analyzed through a spreadsheet program.

2.2. Design of array scanning device

2.2.1. Linear motion slide actuator

A major device that will move the array detector over the test area acted like a mechanical arm in a Cartesian robot (X-Y) [18], [19]. The authors desired to apply it to move only in the X-axis. The characteristic of the linear motion by lead screw slide (DTX0808-400) based on the slide stroke of 400 mm, pitch distance of 5 rev/cm, accuracy of 0.1 mm, step angle of 1.8° and speed of 1-50 mm/s. Therefore, when the motor rotated 1 turn, the linear slide actuator will move 8 mm.

2.2.2. Motor and driver unit

In this article, two phase stepper motors model 17HS8401 (12V 0.55N.m 1.7A 1.8 degrees per step, 200 steps per round) were used to drive a linear slide actuator. Stepper motor was controlled by driver module TB6600, rated current up to 4 A, accepted input voltage in the 9-40V band, the resolution can be adjusted in 1 to 1/32 steps.

A preliminary experiment was conducted to determine the maximum frequency of the square pulse signal for the driver module, which was 1.67 kHz. The basic details were the ball screw of 5 rev/cm, lead screw=(rev/cm)×(1/micro-step)×(360°/step angle)=(5 rev/cm)×(1/2)×(360°/1.8 pulse/rev). Number of pulses per cm was 500 pulse/cm. The pulse frequency was setup to 1.67 kHz, so the movement time in 1 cm was about 300 ms (1 cm=(500 pulse/cm)/(1/0.6 pulse/ms)=300 ms/cm). Therefore, this driver could adjust the pulse frequency appropriately.

2.2.3. Array of photo detector

To measure the non-uniformity of the solar simulator, the TEMT6000 (Vishay) light intensity sensor was used. The TEMT6000 is sensitive to the visible spectrum to near infrared covered range of 360 to 970 nm. The others are the wide angle of ± 60° and the collector light current of 10 μA at the Ev=20 lx. The phototransistor and photodiode provided the best uniformity of light receptors that can convert light intensity into current signals [20]. TEMT6000 is widely used in light intensity measurement and control, such as lighting systems, and measurement systems for greenhouses [21], [22]. The array of photodetector was shown in Figure 1. It consisted of the eight TEMT6000. The sensor was mounted on an aluminum rail. Each sensor could be repositioned to suit for each test area size. Adjusting the position of the photo sensor (sensor 1-8) followed the test area size by moving the sensor on the rail. The distance between the sensor centers was 19.5 mm, 20.75 mm, and 25.5 mm for the test area size of M0 (156×156 mm), M6 (166×166 mm) and M10 (200×200 mm), respectively. The top of the photo detector was covered with a white acrylic to prevent saturation of the photo current of the sensor when it was operated at high light intensity.

All equipments of this array detector scanning system were described in Table 1. It showed the characteristic of each device. The main devices were motor, actuator, photo detector, and controller. It was also presented the dimension of this system.

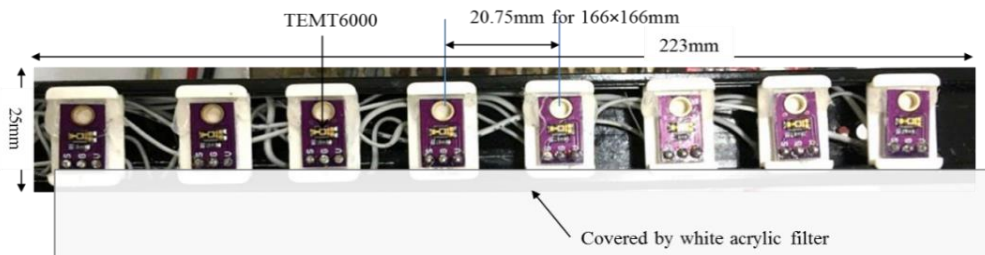


Figure 1. The array of photo detector using eight TEMT6000 photodiode sensors

Table 1. The main characteristic of an array detector scanning device

Device	Detail
Photo detector element	TEMT6000 (Vishay), covered wavelength range of 360 nm to 970 nm.
Array detector dimension	19.5 mm × 20.75 mm × 25.5 mm included 8 of TEMT6000.
Micro-controller and data storage	Arduino Mega2560 with SD card and LCD display.
Array scanning system	Single axis-double direction, desktop type.
Test plan size	156 mm × 156 mm (M0) to 200 mm × 200 mm (M10)
Scanning speed	20.80 s (156 mm × 156 mm), 21.80 s (166 mm × 166 mm), 25.5s (200 mm × 200 mm)
Motor	Stepping-motor model 17HS8410 (12V,0.55Nm, 1.7A, 1.8°/step, controller unit model TB6600)
Linear motion slide actuator	Model DTX0808-400 (slide stroke 400 mm, pitch 5 rev/cm, accuracy 0.1 mm, speed 1 to 50 mm/s)
Device dimension	300 mm × 505 mm × 90 mm

2.3. System block diagram

The test area was divided into 64 cells equally according to the IEC 60904-9 [3]. The measurement locations were defined for row 1-8 and column 1-8 as shown in Figure 2. For example, Array 1/8 was the 1st row and the 8th column. The position of the 8 photo sensors (sensors 1-8) was adjusted according to the size of the test area. The adjustment method was to move the sensor on the rail to 3 different distances (explain in the previous section). The photo sensor in a given position will transmit data from the sensor via an analog to digital (A/D) converter to the input of the Arduino Mega2560 [23]. This device was operated by a switch. To select each test area size, 3 sizes; the position of the sensor was controlled to move relatively to the test area. The motor drive unit received the frequency pulse that generated from microcontroller and the moving speed will be varied by the pulse frequency. All measurement results were collected and stored in the system memory and displayed later. The prototype, in Figure 1, of a non-uniformity measurement by array detector scanning system was shown as CAD design in Figure 3.

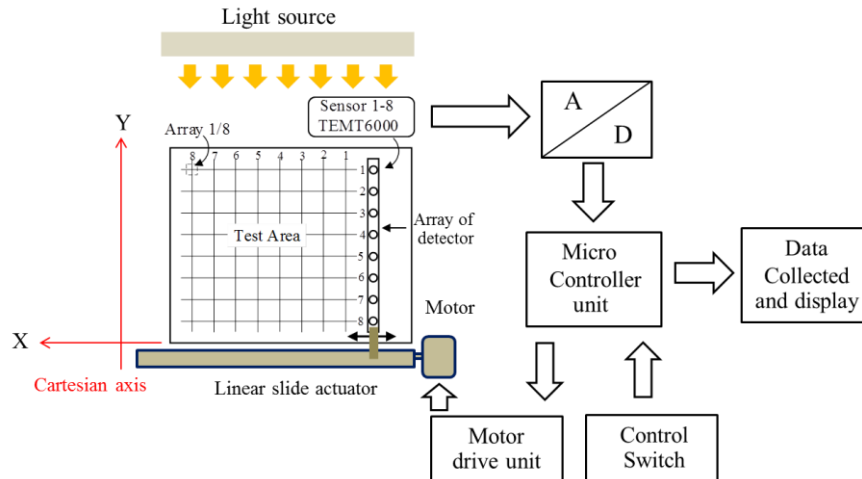


Figure 2. A block diagram of the array detector scanning system

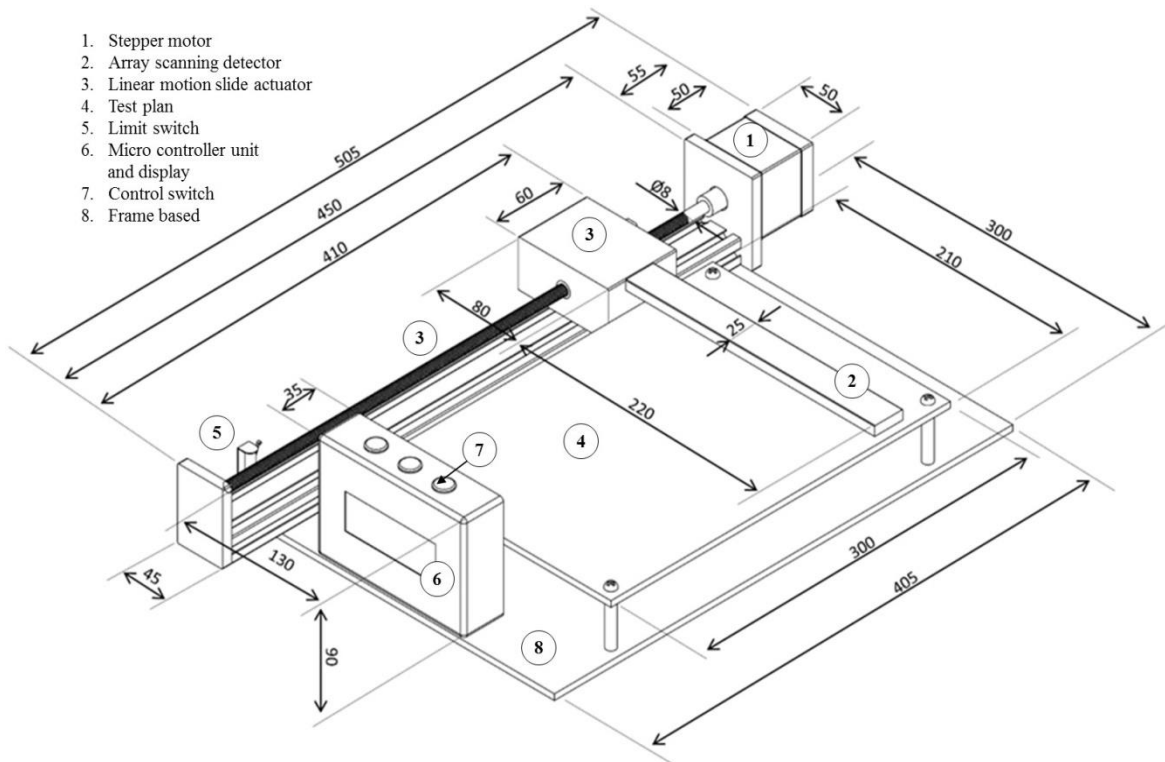


Figure 3. The CAD design of a prototype of a non-uniformity measurement by array detector scanning system (unit: mm.)

2.4. Prototype calibration

The proposed array detector scanning was applied for the steady state solar simulator. The prototype was calibrated in the laboratory at 27 ± 2 °C, and to calibrate the photodiode detector (TEMT6000) with a CMP3 pyranometer (Kipp&Zonen, Germany) under a 200 W luminaire LED light at an irradiance of 100 to 200 W/m². This was due to the limitation of our laboratory that did not have a solar simulator with a light area of 200×200 mm. Each photodetector was calibrated by finding the appropriate multiplier factor and multiplying the light intensity measured by each photodetector. By adding the multiplier factor to the developed compensation program, the program processed the measured light value to match the value of the pyranometer as much as possible.

2.5. Program flowchart of the control scheme

According to Figure 4, the program was started with configuring various variables (configured variables), such as setting the initial traveled distance and defining storage variables. Next, the array detector moved to initial position by setting as a home position and waited for commands from both switches. A command switch, SW1 was to start the movement of an array detector over the test area. A SW2 was to select the size of the test area. The program was designed to select the test area in 3 dimensions of 156×156 mm, 166×166 mm, and 200×200 mm. It was operated by subprogram, namely, size A, size B, and size C, respectively (default s=0). For example, subprogram size A, after SW1 was pushed to start, this subprogram would define the movement step and initialize data of sensors (0-7). Next, the array detector arm moved to the home position and move to 8 positions (step by step). The photodetectors measured and saved the data. Then, the arm would move back to the home position. At each measurement position, the sensor received the light intensity of 3 records (sampling time was 250 ms) and stored the data. The program would take the data from each position to calculate the average of the light intensity at that position (in W/m² and lux). It was displayed on 64 pixels (8×8 positions). Then, the arm would move back to the starting point. Our system was ready to receive orders from the next switch. The size B and size C subprograms had the same procedure. There will only be a different set of moving distance (step). The above operation was shown as flowchart in Figure 4.

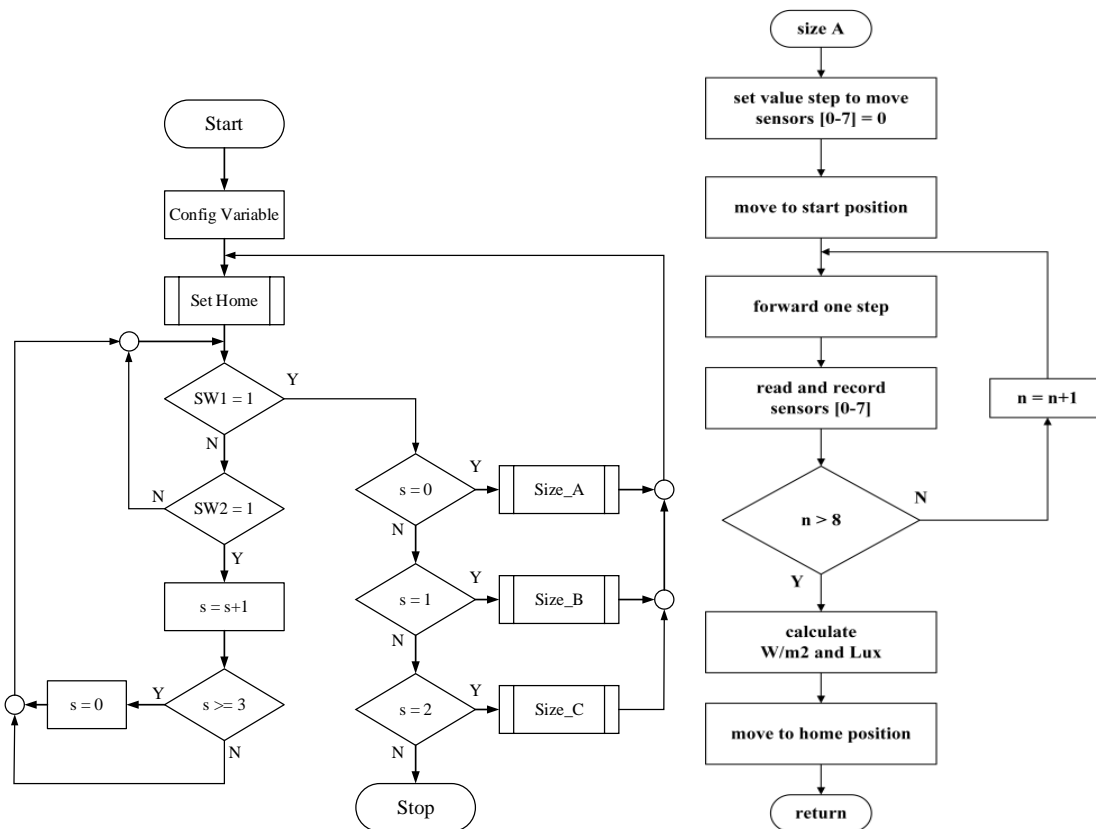


Figure 4. A program flowchart of the movement control of the array detector scanning system

2.6. Experimental procedure

The first goal of this study was to design and construct an array detector scanning system. The authors reported on the development of an array detector scanning system by identifying the physical characteristics. The control and monitor of the system and the movement speed of the array detector were compatible to the design goal. The results of scanning time and scanning speed studies were presented in this section.

The aim of this research was to find out the optimal scanning time to achieve the lowest uncertainty of the measurement. The first experiment, the six of T8 white LED of 23 watts 4,000K was the light source because it could emit the white light covered broadband wavelength. The light source was installed at the center of the test area with a distance from the LED luminaire of 30 cm. The parameters of the light source

included CCT of 3884K, illuminance of 15,383 lx, and peak wavelength of 595 nm (measured by lighting passport spectroradiometer, Essentek, Taiwan). The author chose to do the experiment on the test area of M6 (166mm×166mm) because it was a medium size of the standard solar cell. According to the specific characteristic of linear slide based (Section 2.1), the authors programmed the pulse signal frequency of 1.67 kHz, 1.25 kHz, and 1.00 kHz to obtain an estimated scanning time of 17.96 s, 21.8 s and 24.6 s, respectively (Table 2). Light irradiance was measured and recorded of three rounds at each scanning time. The equation that used for estimating speed and time was shown in (1) and (2).

$$\text{Moving speed (mm/s)} = \frac{d_p}{n_s} \times \frac{1000}{T} \quad (1)$$

$$\text{Moving time (s)} = \frac{2d_T}{\text{moving speed}} \quad (2)$$

where; n_s =number of step between the measurement position (1037.5 steps); d_p =distance between measurement position (20.75 mm in case of test area of 166×166 mm); and $T=1/f_p$, f_p =signal pulse frequency (kHz), d_T = total moving distance (166 mm). Measurement time was the estimated stop time of photodetector array and measured in one round of scanning (1 s per 1 position so total was 8 s).

The non-uniformity and uncertainty were calculated by using (3), (4) and (5) [2], [24], [25]. Because this study applied to the same prototype that was used in the experiment, the systemic errors such as error of photo detector, micro-controller, A/D converter, and linear slide based occurring in all experiments could be estimated to be equal. Analysis of Type-B of uncertainty could, therefore, be omitted from the analysis. A method that used for determining the uncertainty was the statistical analysis of Type-A. “The Type-A standard uncertainty is obtained from a probability density function derived from an observed frequency distribution” [24]. The uncertainty Type-A was suitable for analysis in this study. The results of the study were detailed in the results and discussion section.

$$\text{non - uniformity} = \left[\frac{\text{max} - \text{min}}{\text{max} + \text{min}} \right] \times 100\% \quad (3)$$

where *max* was a maximum irradiance, *min* was a minimum irradiance by measurement results.

$$\text{uncertainty}(u_A) = \sqrt{\frac{\sum_{i=1}^n (x_i - \bar{x})^2}{n \times (n-1)}} \quad (4)$$

$$\% \text{uncertainty} (\%u_A) = \frac{u_A}{\bar{x}} \times 100\% \quad (5)$$

where x_i was measurement of non-uniformity of $i=1, 2, 3, \dots, n$ and \bar{x} was an arithmetic mean of the non-uniformity. The u_A was a Type-A uncertainty and $\%u_A$ was Type-A percentage of uncertainty.

$$\text{MAE} = \frac{\sum_{i=1}^n |\text{error}|}{n} \quad (6)$$

where *MAE*= mean absolute error, *error* = measurement value – reference value, n = number of data.

To study of the non-uniformity of irradiance on the difference test plane, the system was shown in Figure 5. In the second experiment, the authors applied the scanning time with the least uncertainty to non-uniformity measurements on three different test plans. There are 156×156 mm, 166×166 mm, and 200×200 mm by using the same light intensity of light sources as the first experiment. The authors repeated the experiment, a total of three times, to minimize potential discrepancies. Then, the measurement results were compared with the non-uniformity that measured by using a single detector (Figure 5(a)). The MAE for each case was evaluated by (6) [26]. In this study, a pyrometer model CMP3 (Kipp&Zonen, Germany) was used as a single detector.

Table 2. Signal pulse frequency and total estimated time based on test area of 166mm ×166mm

Signal pulse frequency(kHz)	Moving speed (mm/sec)	Moving time(s)	Measurement time(s)	Total estimated time(s)
1.67	33.33	9.96	16.00	26
1.25	24.00	13.80	16.00	30
1.00	20.00	16.60	16.00	33

3. RESULTS AND DISCUSSION

3.1. Development of an array detector scanning system

The non-uniformity of irradiance measuring device developed by the authors was a bench top type with dimensions of 30×55×15 cm. It was suitable for applying to test irradiance from a light source mounted on top of the prototype. The base of the test area had dimensions of 210×297 mm. The location of the light sensor inside the array detector can be adjusted by a total exposure distance between 150 mm to 200 mm as shown in Figure 4. The dimension of the test area and the operating speed were selected through a control's program. It was suitable for using in steady-state solar simulators with a light area of no more than 200×200 mm. The comparative results of scanning time when adjusted for scanning speed of fast (33.33 mm/s), medium (24.00 mm/s), and slow (20.00 mm/s) were found that it was compatible with the results of the calculations.

Two limit switches were installed in the system as a protection switch at the start and stop position of a linear actuator. It made sure that the array scanning bar would be stopped after moving to these positions. The system controlled the movement of the linear actuator to a given position. The authors developed by not requiring a feedback position control system. The authors chose the stepping motor rotation control method as a positioning technique which was suitable, simple, and uncomplicated for software and hardware design (described in Section 2). The LCD display showed the operating status, time, and position of our prototype. After testing the functionality of prototype by observing the stop of the array detector bar at any position, the accuracy of this system was satisfied. It was corresponded to the movement of Cartesian robot of Raja *et al.* [18].

According to Table 3, the results showed that the scanning time was slightly higher than the calculated result. By the way, at fast, medium, and slow speeds, the experimental results obtained 2.43 s, 1.59 s, and 1.76 s, respectively. The analysis made sense because the movement time depended on the motor speed in conjunction with the mechanical drive, which increased the travelling time due to friction loss of the ball screw and other mechanical movement. For an electrical part, there may be a motor's loss and a delay time of the limit switch. The delay time might cause by an operation between the software program and controller.

Table 3. Experimental results of the scanning time

Signal pulse Frequency (kHz)	Scanning speed	Scanning time (s)		
		Calculation	Experiment	Difference
1.67	Fast	17.96	20.39	2.43
1.25	Medium	21.80	23.39	1.59
1.00	Slow	24.60	26.36	1.76

3.2. The optimal scanning time

The authors performed an experiment to analyze the optimal scanning time of non-uniformity measurement on the test area of 166mm×166mm using our prototype as Figure 5(b). The experiment was set to measure three times in each scanning speed as fast, medium, and slow of 20.39 s, 23.39 s, and 26.36 s, respectively. Details were shown in Table 3. The analysis results of non-uniformity's measurement at each speed were shown in Figure 6.

At the fast speed, in Figure 6, the average non-uniformity was 8.28% (8.23, 8.23, and 8.39%). At the medium and low speed, the average non-uniformity results were 8.20% (8.21, 8.09, and 8.31%) and 8.73% (9.62, 8.21, and 8.36%), respectively. The most distribution was at lowest scanning speed (26.36 s/round), then, followed by 23.39 and 20.39 s/round. These results were affected to the different estimate of measurement uncertainty. The optimal speed analysis was used to control the movement of array detector scanning device to measure the light presented by the authors. The analysis was based on the time with the lowest uncertainty. The uncertainty was analyzed by (3) and (4) and the analysis results were presented in Table 4.

The results of Table 4 showed the non-uniformity analyzed from the light intensity measurements presented by the authors at the three scanning speeds. It offered that the non-uniformity almost equal at the fast and medium speed, the scan times of 20.39s and 23.39s. It was more stable than scanning with longer times, as 26.36s. The experimental results offered that percentage of uncertainty at the fast, medium and low scanning speed were 0.59% (0.08), 0.79% (0.11), and 5.14% (0.78), respectively. This showed that the optimum scanning time with the lowest uncertainty was a fast speed of 20.39 s/round or 33.33 mm/s. In further experiments under section 3.3, the authors programmed a pulse frequency of 1.67 kHz to obtain a moving speed of 33.33 mm/s. This is the speed that tends to result in discrepancy minimal.

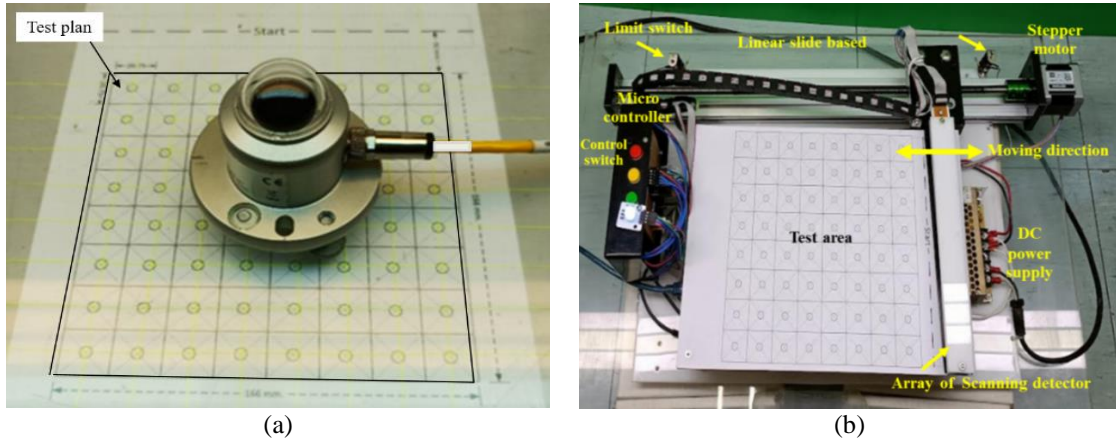


Figure 5. A single detector and a proposed array detector prototype. (a) A pyrometer model CMP3 as a single detector in traditional measurement methods and (b) The prototype of non-uniformity measurement by array detector scanning system (top view)

Fast speed 20.39s (1.67 kHz)

Round 1 Unit W/m²

41.7	44.1	44.6	42.1	44	40.7	41.2	40.5
42.5	44.6	45.3	42.8	44.9	41.4	41.8	41.2
42.8	45	45.6	43.1	45.5	41.7	42.2	41.7
42.8	45.1	45.7	42.9	45.5	42	42.2	41.5
42.3	44.8	45.5	42.8	45	41.4	42.1	41.6
41.8	44.1	44.8	42.1	44.6	40.9	41.5	40.9
40.9	43.2	43.9	41.4	43.4	40.2	40.6	40.2
39.8	42	42.5	40.1	42.2	38.8	39.3	39.1

max=45.7 min=38.8 SD=1.81
non-uniformity=8.23%

Round 2

41.7	44.1	44.6	42.1	44	40.7	41.2	40.5
42.5	44.6	45.3	42.8	44.9	41.4	41.8	41.2
42.8	45	45.6	43.1	45.5	41.7	42.2	41.7
42.8	45.1	45.7	42.9	45.5	42	42.2	41.5
42.3	44.8	45.5	42.8	45	41.4	42.1	41.6
41.8	44.1	44.8	42.1	44.6	40.9	41.5	40.9
40.9	43.2	43.9	41.4	43.4	40.2	40.6	40.2
39.8	42	42.5	40.1	42.2	38.8	39.3	39.1

max=45.7 min=38.8 SD=1.81
non-uniformity=8.23%

Round 3

41.7	44.2	44.7	42.1	44.3	40.7	41.3	40.6
42.5	44.8	45.5	42.9	44.9	41.5	41.8	41.3
42.9	45	45.7	43.1	45.4	41.8	42.1	41.7
42.6	45.1	45.5	42.9	45	41.5	42	41.6
42.2	44.7	45.4	42.6	44.8	41.4	42.2	41.4
41.7	44	44.7	42.2	44.1	40.7	41.4	40.8
40.8	43.1	43.5	41.2	43.2	40	40.5	40.1
39.7	41.7	42.4	40.1	42.2	38.9	39.2	39.1

max=45.7 min=38.9 SD=1.80
non-uniformity=8.39%

Medium speed 23.39s (1.25 kHz)

Round 1 Unit W/m²

41.7	44	44.7	42.1	44.1	40.8	41.3	40.6
42.4	44.9	45.5	42.8	45	41.2	41.6	41.2
42.8	45.3	45.8	43.1	45.3	41.6	42.1	41.7
42.9	45	45.7	43	45.4	41.7	42.4	41.8
42.8	44.9	45.5	42.8	45	41.5	42.1	41.8
42.1	44.1	44.7	42.2	44.5	40.8	41.5	41.3
40.8	43.2	43.9	41.4	43.3	40.1	40.6	40
39.8	42	42.6	40.1	42.3	38.9	39.4	39.1

max=45.8 min=38.9 SD=1.82
non-uniformity=8.21%

Round 2

41.7	44	44.6	42.2	44	40.7	41	40.6
42.5	44.9	45.3	42.8	44.9	41.5	42	41.2
42.6	45.1	45.6	43	45.3	41.7	42.2	41.7
42.8	45	45.7	42.9	45.1	41.8	42.1	41.6
42.4	44.7	45.5	42.6	44.9	41.4	41.8	41.3
41.7	43.9	44.5	41.8	44.1	40.7	41.2	40.7
40.7	42.9	43.5	41.2	43.1	39.7	40.7	39.8
39.7	41.7	42.4	40.1	42.1	38.9	39.7	39.1

max=45.7 min=38.9 SD=1.80
non-uniformity=8.09%

Round 3

41.8	44.1	44.8	42.3	44.1	40.8	41.3	40.7
42.4	44.7	45.4	42.8	45	41.5	42	41.2
43	45.4	46.1	43.1	45.6	41.8	42.4	41.8
43	45.1	45.8	43.1	45.4	42	42.4	42
42.5	44.9	45.6	42.8	45	41.4	42.2	41.6
41.7	44.2	44.7	42.2	44.2	40.8	41.4	41
40.8	43.2	43.5	41.2	43.3	40	40.5	40.1
39.8	41.8	42.5	40.2	42.2	39.3	39.4	39

max=46.1 min=39.9 SD=1.32
non-uniformity=8.31%

Low speed of 26.36s (1.00 kHz)

Round 1 Unit W/m²

38.5	41.4	42.1	39.9	41.7	37.6	37.7	38.9
39.8	42.8	43.4	41.2	43.1	39	39.2	40
40.6	43.8	44.2	42	44.1	39.8	40.1	40.7
40.7	43.8	44.8	42	44.5	40	40.7	40.9
40.7	43.5	44.3	42	44.1	39.7	40.4	40.9
39.9	43	43.9	41.4	43.9	39.2	39.9	40.5
38.8	41.6	42.3	40.2	42.3	38.2	39	39.3
37.4	40.1	40.8	39	40.9	36.9	37.5	38.1

max=44.8 min=36.9 SD=2.04
non-uniformity=9.62%

Round 2

42	44.6	44.9	42.4	44.7	40.9	41.6	40.7
42.6	45	45.8	42.9	45.3	41.6	42	41.3
42.9	45.3	45.8	43.2	45.5	41.8	42.4	41.7
42.9	45.1	45.8	43.1	45.4	41.7	42.3	41.7
42.6	45.1	45.8	42.9	45.4	41.5	42.2	41.6
42	44.2	44.9	42.4	44.6	40.8	41.5	41
40.9	43.3	44	41.4	43.5	40.1	40.6	40.2
39.9	41.8	42.5	40.2	42.3	38.9	39.6	39.2

max=45.8 min=38.9 SD=1.87
non-uniformity=8.21%

Round 3

41.7	44	44.7	42.2	44.3	40.6	41	40.4
42.4	44.5	45.4	42.8	44.9	41.4	41.6	41
42.9	45.3	45.8	43.2	45.3	41.7	42.1	41.7
42.9	45	45.7	43.2	45.5	41.7	42.1	41.8
42.3	44.7	45.5	42.6	44.8	41.2	42	41.5
41.6	44.2	44.9	42	44.6	40.6	41.2	40.6
40.7	43	43.8	41.2	43.3	39.9	40.6	40
39.4	41.8	42.5	40	42.4	38.8	39.3	38.9

max=45.8 min=38.8 SD=1.88
non-uniformity=8.36%

Figure 6. Measurement results of irradiance by an array detector scanning system under different scanning time

Table 4. The analysis results of the uncertainty of the non-uniformity measurement by the array detector scanning system

Items	Moving speed			Unit
	Fast	Medium	Slow	
Round 1	8.23	8.21	9.62	W/m ²
Round 2	8.23	8.09	8.21	
Round 3	8.09	8.31	8.36	
Average	8.18	8.20	8.73	
Uncertainty	0.05	0.06	0.45	
Deviation	0.08	0.11	0.78	-
% Uncertainty	0.59	0.79	5.14	%

3.3. The analysis of the non-uniformity of irradiance

The scanning time of our proposed system was set at the fast speed of 33.33 mm/s. The experimental procedure was described in the section 3.2. The mean absolute error (MAE) of the results between two methods had to analyze [22], [27]. The results of the non-uniformity of irradiance on different test area and the array scanning time of our prototype were shown in Table 5 and 6.

In Table 5, the measurement results of non-uniformity with a single detector at test area of 156 × 156, 166×166 and 200×200 (mm×mm) were 6.39%, 6.45%, and 7.69%, respectively. The results for the array scanning system at the same area were 7.63%, 7.29%, and 9.35%, respectively. From the experiment, the non-uniformity that obtained from the array detector scanning system was different from the single detector method. When analysing the mean error by comparing the measurement results with a single detector, mean absolute error was 1.27 of the reference (single detector method). However, the measurement by any means, its value increased as the size of the test area always increased whether the distance to the light source was constant. This was reasonable because the size of the test area was larger using the same light source. The light intensity around the test area would decrease the non-uniformity of solar simulator as [1], [2], [10], [14], and [28].

Table 5. The analysis results of non-uniformity comparison between single-detector and our array scanning system

Test area (mm×mm)	Non-uniformity (%)						MAE
	Single detector			Array scanning system			
	mean	SD	% uncertainty	mean	SD	% uncertainty	
156×156	6.39	0.65	5.84	7.63	0.21	1.60	1.23
166×166	6.45	0.75	6.71	7.29	0.15	1.19	0.92
200×200	7.69	0.64	4.81	9.35	0.23	1.43	1.66

Table 6. The analysis results of measurement time comparison between single-detector and our array scanning system (n=3)

Test area (mm×mm)	Measurement time (s)				Time ratio
	Single detector		Array scanning system		
	mean	SD	mean	SD	
156×156	714.00	0.30	20.80	0.02	34
166×166	735.40	0.21	21.80	0.07	33
200×200	746.40	0.13	25.51	0.04	29

However, the experimental results were shown that the array detector scanning system measurements were more reliable because each measurement result in the same test-area were %uncertainty in average of 1.41% lower than that of the single detector (5.79%) significantly. The non-uniformity of irradiance on the test area was different from a single detector, possibly due to several reasons. For example: i) the pyranometer was used as a single detector that presented the measurement results only an integer number so it did not show the decimal point; ii) The single detector measurement took a longer time (10-12 min) compared to the proposed method. The temperature effect, the measurement placement discrepancies, and human errors might include in measurement results with greater uncertainty; iii) The possible errors in irradiance calculation with equations derived from experimental results to create a fit-curve might increase the errors.

The Table 6, the non-uniformity’s measurement method with the array scanning system indicated that the measurement time was 20.80 s, 21.80 s, and 25.51 s on the test area of 156×156, 166×166, and 200×200 mm, respectively. When measuring with the traditional method, the measured time was 32 times longer (mean) than our method. The highlight of this method was that the average measurement time was

only 1 of 32 of the time measured by a single detector on all test areas. Our prototype, the distance of each photo detector could be adjusted suitably to different test areas without having to update the driver. While 64 photodiodes array detectors, despite their best measurement speed and uncertainty [13]-[14], can only be used for a test area of any size, the non-uniformity measurement by the proposed array detector scanning system was an interesting approach. It provided a measurement result with lower percentage of uncertainty than a single detector measurement method. Measurement accuracy was acceptable. The measurement time was very low, only 1 of 32 of the single detector measurement time.

4. CONCLUSION

The array detector consisted of eight-photodiode detector. Authors applied a linear slide base as a mechanism to move the array detector sweeping across the plane of the lighting area. To measure the light irradiance in 64 positions according to the non-uniformity of irradiance was specified in standard IEC 60904-9. The proposed measurement system used a single scan to measure 64 points and took less than 26 s scan time on a 200×200 mm exposure area. The signal pulse frequency for stepper motor driver was 1.67 kHz that was the optimal frequency because the uncertainty of measurement was lowest. The percentage of uncertainty of the measurement in average is 1.41% lower than the traditional method. When the non-uniformity measurement was used on the difference test area, the results indicated that the MAE of the proposed system was equal to 1.27 from the traditional method. However, the measurement time was only 1 of 32 of the traditional method and the uncertainty was clearly better. The advantage of this prototype was also presented here. The distance of the photodetector could be precisely adjusted to suit the test area of 156×156mm to 200×200 mm. This concept can be applied to develop a non-uniformity measurement system for the solar simulator for PV module applications. The possible future study, the authors should develop a prototype that will capably measure artificial irradiance of 1000 W/m² and a program to calculate the non-uniformity and create the 3D uniformity map immediately.

ACKNOWLEDGEMENTS

The authors would like to thank Rajamangala University of Technology Suvarnabhumi for supporting the budget and equipment's in the laboratory. This work was accomplished for its intended purpose.




REFERENCES

- [1] N. Watjanatepin and P. Sritanauthaikorn, "Rectangular module for large scale solar simulator based on high-powered LEDs array," *Telkomnika (Telecommunication Computing Electronics and Control)*, vol. 20, no. 2, pp. 462–474, Apr. 2022, doi: 10.12928/TELKOMNIKA.v20i2.23308.
- [2] N. Watjanatepin, "Design Construct and Evaluation of Six- Spectral LEDs-Based Solar Simulator Based on IEC 60904-9," *International Journal of Engineering and Technology*, vol. 9, no. 2, pp. 923–931, Apr. 2017, doi: 10.21817/ijet/2017/v9i2/170902101.
- [3] IEC, "Photovoltaic devices -- Part 9: Solar simulator performance requirements," in *Photovoltaic devices— Part 9: Solar Simulator Performance requirements*, 2007, pp. 1–15.
- [4] D. I. Paul, M. Smyth, A. Zacharopoulos, and J. Mondol, "The effects of nonuniform illumination on the electrical performance of a single conventional photovoltaic cell," *International Journal of Photoenergy*, vol. 2015, pp. 1–10, 2015, doi: 10.1155/2015/631953.
- [5] M. H. Al-Jumaili, A. S. Abdalkafor, and M. Q. Taha, "Analysis of the hard and soft shading impact on photovoltaic module performance using solar module tester," *International Journal of Power Electronics and Drive Systems (IJPEDS)*, vol. 10, no. 2, p. 1014, Jun. 2019, doi: 10.11591/ijpeds.v10.i2.pp1014-1021.
- [6] A. H. Numan, Z. S. Dawood, and H. A. Hussein, "Theoretical and experimental analysis of photovoltaic module characteristics under different partial shading conditions," *International Journal of Power Electronics and Drive Systems*, vol. 11, no. 3, pp. 1508–1518, Sep. 2020, doi: 10.11591/ijpeds.v11.i3.pp1508-1518.
- [7] R. Herrero, M. Victoria, C. Dominguez, S. Askins, I. Antón, and G. Sala, "Understanding causes and effects of non-uniform light distributions on multi-junction solar cells: Procedures for estimating efficiency losses," in *AIP Conference Proceedings*, 2015, vol. 1679, p. 050006, doi: 10.1063/1.4931527.
- [8] E. Yandri, "Uniformity characteristic and calibration of simple low cost compact halogen solar simulator for indoor experiments," *International Journal of Low-Carbon Technologies*, vol. 13, no. 3, pp. 218–230, Sep. 2018, doi: 10.1093/IJLCT/CTY018.
- [9] V. Esen, S. Saglam, B. Oral, and O. C. Esen, "Toward Class AAA LED Large Scale Solar Simulator with Active Cooling System for PV Module Tests," *IEEE Journal of Photovoltaics*, vol. 12, no. 1, pp. 364–371, Jan. 2022, doi: 10.1109/JPHOTOV.2021.3117912.
- [10] C. A. Matias *et al.*, "Optimized Solar Simulator Structure for Uniform Irradiance Distribution," in *Proceedings - 2018 IEEE International Conference on Environment and Electrical Engineering and 2018 IEEE Industrial and Commercial Power Systems Europe, IEEEIC/ and CPS Europe 2018*, Jun. 2018, pp. 1–6, doi: 10.1109/IEEEIC.2018.8494430.
- [11] D. Colarossi, E. Tagliolini, P. Principi, and R. Fioretti, "Design and validation of an adjustable large-scale solar simulator," *Applied Sciences (Switzerland)*, vol. 11, no. 4, pp. 1–13, Feb. 2021, doi: 10.3390/app11041964.
- [12] Y. He, L. Xiong, H. Meng, J. Zhang, D. Liu, and J. Zhang, "Analysis of non-uniformity of irradiance measurement uncertainties of a pulsed solar simulator," in *Optical Metrology and Inspection for Industrial Applications II*, Nov. 2012, vol. 8563, p. 856318, doi: 10.1117/12.981437.

- [13] M. Mittag, A. Pfreundt, and J. Shahid, "Impact of Solar Cell Dimensions on Module Power, Efficiency and Cell-To-Module Losses," in *Proceedings of the 30th PV Solar Energy Conference (PVSEC-30)*, 2020, pp. 1–6.
- [14] D. Rivola, S. Dittmann, M. Pravettoni, G. Friesen, and D. Chianese, "High-speed multi-channel system for solar simulator irradiance non-uniformity measurement," in *2014 IEEE 40th Photovoltaic Specialist Conference (PVSC)*, Jun. 2014, pp. 2611–2615, doi: 10.1109/PVSC.2014.6925465.
- [15] Y. Yuan, Y. Yang, and Y. Zhang, "Research of solar simulator irradiance non-uniformity measurement," in *Proceedings - IEEE 2011 10th International Conference on Electronic Measurement and Instruments, ICEMI 2011*, Aug. 2011, vol. 3, pp. 307–310, doi: 10.1109/ICEMI.2011.6037912.
- [16] R. Jintamethasawat *et al.*, "Non-uniformity Correction Algorithm for THz Array Detectors in High-Resolution Imaging Applications," *Journal of Infrared, Millimeter, and Terahertz Waves*, vol. 41, no. 8, pp. 940–956, Aug. 2020, doi: 10.1007/s10762-020-00698-y.
- [17] Z. Eshaghi, "Photodiode Array Detection in Clinical Applications; Quantitative Analyte Assay Advantages, Limitations and Disadvantages," in *Photodiodes - Communications, Bio-Sensings, Measurements and High-Energy Physics*, InTech, 2011.
- [18] V. Raja, B. Bhaskaran, K. K. G. Nagaraj, J. G. Sampathkumar, and S. R. Senthilkumar, "Agricultural harvesting using integrated robot system," *Indonesian Journal of Electrical Engineering and Computer Science*, vol. 25, no. 1, pp. 152–158, Jan. 2022, doi: 10.11591/ijeecs.v25.i1.pp152-158.
- [19] S. Nakdhamabhorn and J. Suthakorn, "System integration of a fluoroscopic image calibration using robot assisted surgical guidance for distal locking process in closed intramedullary nailing of femur," *International Journal of Electrical and Computer Engineering (IJECE)*, vol. 9, no. 5, p. 3739, Oct. 2019, doi: 10.11591/ijece.v9i5.pp3739-3750.
- [20] J. Liu, B. Z. Zhang, H. Liu, S. S. Zeng, W. Q. Zhao, and L. G. Lu, "Impact of detector spatial uniformity on the measurement of averaged led intensity," *IEEE Photonics Journal*, vol. 6, no. 1, pp. 1–7, Feb. 2014, doi: 10.1109/JPHOT.2013.2295458.
- [21] E. Romano, M. Brambilla, P. Toscano, and C. Bisaglia, "A Method to Implement a Monitoring System Based on Low-Cost Sensors for Micro-environmental Conditions Monitoring in Greenhouses," in *Lecture Notes in Civil Engineering*, vol. 67, 2020, pp. 775–782.
- [22] P. N. S. M. Mustafa, A. S. Azam, M. S. Sulaiman, A. F. Omar, and M. F. A. Rahman, "Development of an optical pH measurement system based on colorimetric effect," *Indonesian Journal of Electrical Engineering and Computer Science*, vol. 24, no. 2, p. 728, Nov. 2021, doi: 10.11591/ijeecs.v24.i2.pp728-735.
- [23] S. H. Yusoff, S. Mahat, N. S. Midi, S. Y. Mohamad, and S. A. Zaini, "Classification of different types of metal from recyclable household waste for automatic waste separation system," *Bulletin of Electrical Engineering and Informatics*, vol. 8, no. 2, pp. 488–498, 2019, doi: 10.11591/eei.v8i2.1488.
- [24] F. Sametoglu, "Evaluation of expanded uncertainties in luminous intensity and illuminance calibrations," *Applied Optics*, vol. 47, no. 31, pp. 5829–5847, 2008, doi: 10.1364/AO.47.005829.
- [25] M. N. Ibrahim, Z. H. C. Soh, N. S. M. Hadis, and A. Othman, "Uncertainty and sensitivity analysis applied to a voltage series operational amplifier," *Indonesian Journal of Electrical Engineering and Computer Science*, vol. 21, no. 3, p. 1347, Mar. 2021, doi: 10.11591/ijeecs.v21.i3.pp1347-1355.
- [26] W. Wang and Y. Lu, "Analysis of the Mean Absolute Error (MAE) and the Root Mean Square Error (RMSE) in Assessing Rounding Model," *IOP Conference Series: Materials Science and Engineering*, vol. 324, no. 1, 2018, doi: 10.1088/1757-899X/324/1/012049.
- [27] H. Suyono, R. N. Hasanah, R. A. Setyawan, P. Mudjirahardjo, A. Wijoyo, and I. Musirin, "Comparison of solar radiation intensity forecasting using ANFIS and multiple linear regression methods," *Bulletin of Electrical Engineering and Informatics*, vol. 7, no. 2, pp. 191–198, Jun. 2018, doi: 10.11591/eei.v7i2.1178.
- [28] A. Al-Ahmad, D. Clark, J. Holdsworth, B. Vaughan, W. Belcher, and P. Dastoor, "An Economic LED Solar Simulator Design," *IEEE Journal of Photovoltaics*, vol. 12, no. 2, pp. 521–525, Mar. 2022, doi: 10.1109/JPHOTOV.2022.3143460.

BIOGRAPHIES OF AUTHORS






Napat Watjanatepin    received the B.S. Tech. Ed. (Electrical Engineering) degree from Institute of Technology Vocational Education, Thailand in 1985, and M.S. Tech. Ed. (Electrical Technology) degree from King Mongkut's Institute of Technology North Bangkok, Thailand in 1991. His research interests include power electronics and drives, renewable energy, PV energy system, LED solar simulator, LED for horticulture and engineering educations. He can be contacted at email: napat.w@rmutsb.ac.th.






Patcharanan Sritanauthaikorn    received the B. Eng. (Electrical Engineering) degree from Khon Kaen University, Thailand in 1998, and M. Eng. (Electrical Engineering) degree from King Mongkut's University of Technology Thonburi, Thailand in 2004. Her research interests include control system, automation, power electronics, renewable energy, and LED solar simulator. She can be contacted at email: patcharanan.s@rmutsb.ac.th.



Chaiyant Boonmee    received his B. Eng in electrical engineering from Rajamangala Institute of Technology Thewes, his M. Eng degrees from Rajamangala University of Technology Thanyaburi and his Ph.D. degree in electrical engineering from Chiang Mai University (CMU), Chiang Mai, Thailand, in 2017. His research interests include power electronic application, multilevel cascaded inverters and IoT application. He can be contacted at email: chaiyant.b@rmutsb.ac.th.






Paiboon Kiatsookkanatorn    received the B.S.Tech.Ed. and B.Eng. degrees from Rajamangala Institute of Technology, Thailand in 1998 and 2002, respectively, and the M.Eng. and Ph.D. degrees from Chulalongkorn University, Bangkok, Thailand in 2005 and 2012, respectively. He is currently an Assistant Professor in the Department of Electrical Engineering, Rajamangala University Suwarnabhumi (RMUTSB), Thailand. His research interests include matrix converters and pulsewidth-modulation (PWM). He can be contacted at email: paiboon.k@rmutsb.ac.th.



Sarayoot Thongkullaphat    received the B.Ind. Tech. (Electrical Engineering) degree from South-East Asia University, Thailand in 1996, M. Eng. (Electrical Engineering) degree from King Mongkut's University of Technology Thonburi, Thailand in 2004, and Ph.D. (Electrical Engineering) degree from King Mongkut's University of Technology North Bangkok, Thailand in 2014. His research interests include power electronics and drives, control system, renewable energy, LED solar simulator, and renewable energy. He can be contacted at email: sarayoot.t@rmutsb.ac.th.



Suvinai Sodajaroen    received his B. Eng. degree in Industrial Engineering from Rajamangala University of Technology Lanna, Thailand in 2009, and M. Eng. degree in Manufacturing Engineering from Rajamangala University of Technology Thanyaburi, Thailand in 2015. His research interests include Computer Aided design (CAD), Production engineering, Material Scien, and Welding Engineering. He can be contacted at email: suvinai.s@rmutsb.ac.th.